Available online at www.sciencedirect.com

ScienceDirect

Physics Procedia 49 (2013) 205 – 216

Physics Procedia

Spintronic Materials: Nanostructures and Devices (SMND-2011)

Synthesis and Characterization of Cobalt doped Manganese Oxide Nanoparticles by Chemical Route

K.S.Pugazhvadivu[a], K.Ramachandran[b] and K.Tamilarasan[a*]

[a]*Thin Film Research Centre, Deartment of Physics, Kongu Engineering College, Perundurai- 638 052, India*

[b]*School of Physics, Madurai Kamaraj University, Madurai-625 021, India*

Abstract

Cobalt doped α-Mn_2O_3 nanoparticles have been synthesized by chemical route. The structural properties were analyzed by X-ray diffraction (XRD) and scanning electron microscope (SEM) analysis. The SEM image shows that the nanoclusters having spherical geometry. The optical properties were analyzed by ultraviolet - visible (UV-Vis) and Fourier transform infrared (FTIR) spectroscopy. UV-Vis spectra illustrates that Co doped Mn_2O_3 nanosystem acquire blue shift from bulk value (2.5 eV). The chemical composition and purity of the samples were examined using energy dispersive analysis of X-ray spectroscopy (EDAX). Magnetic properties were studied using electron paramagnetic resonance (EPR) and Guoy's method. The high magnetic moment of 3.5μB shows the enhancement in magnetic transition temperature (T_c) of Mn_2O_3 nanosystem due to the incorporation of cobalt ions.

Selection and peer-review under responsibility of the Department of Physics, School of Science and Humanities, Kongu Engineering College

Keywords: nanoparticles; Co doped Mn_2O_3; X-ray diffraction; Electron paramagnetic resonance

1. Introduction

Recently metal oxide nanoparticles have been the subject of much interest because of their unusual optical, electronic and magnetic properties, which often differ from the bulk. A large number of different manganese oxides are possible due to the availability of various oxidation states of manganese (II, III, IV). The magnetic properties of manganese oxide nanoparticles are of increasing research interest due to their intrinsic high atomic moment of Mn and its various magnetic alignment [1]. The most commonly known manganese oxides MnO, Mn_2O_3, and Mn_3O_4 have a wide range of applications in catalysis and battery technologies [2, 3]. Polymorphs of Mn_2O_3 have been used as catalyst for removing carbon monoxide, nitrogen oxide from waste gas [4-6]. Researchers have shown considerable interest in the last few years in lithium intercalated Mn_2O_3 as an electrode material for rechargeable lithium batteries [7, 8].

* Corresponding author. Tel.: +914294-226611; fax: +914294-220087.

E-mail address: dr.k.tamilarasan@gmail.com.

Selection and peer-review under responsibility of the Department of Physics, School of Science and Humanities, Kongu Engineering College

doi:10.1016/j.phpro.2013.10.028

In this respect, nano sized Mn_2O_3 is expected to display better performance due to reduction in grain size and increased surface area [9]. It is also used to prepare soft magnetic materials such as manganese, zinc ferrite, which is useful for magnetic cores in transformers for power supplies [10-12]. It is used in the manufacture of welding rods and fluxes. It is one of the raw materials in the manufacture of professional grade ferrites [13]. Various methods have been used for the preparation of nanocrystalline Mn_2O_3 powders such as hydrothermal [14], thermo chemical [15], spray pyrolysis [16], chemical liquid homogeneous precipitation [17], thermal decomposition [3] and arc evaporation [18]. For magnetic storage application, the material should be ferromagnetic. Cobalt is a ferromagnetic material with curie temperature 1393 K. Mn_2O_3 (bulk) is an antiferromagnetic material with Neel temperature 90 K. However, nano Mn_2O_3 has ferromagnetic nature at liquid nitrogen temperature [19]. So that the study of cobalt doped Mn_2O_3 is very interesting one. The goal of this work is to synthesis and characterize α-Mn_2O_3 nanosystems and its magnetic properties by doping Co ions.

2. Synthesis

Manganese acetate tetrahydrate [$Mn(OAc)_2.4H_2O$(99% Aldrich)], N, N'- dimethylformamide, [DMF (99.8% Aldrich)], acetone [CO $(CH_3)_2$(Fermont 99.7%)] and deionised water were used as starting materials. At first 0.03063gm of $Mn(OAc)_2.4H_2O$ was dissolved in DMF (22.5ml) under vigorous stirring, 2.5ml of deionised water was added to get a final concentration of 5×10^{-3}M. The amber solution was stirred at 323 K for 1hour and the resulting solution was left to stand for 3 months under room temperature. After 3 months, the dark brown precipitate was obtained. The obtained precipitate was centrifuged and washed several times with distilled water and acetone to remove excess surfactant from the solution and then dried in air at 353 K for 30 minutes. Cobalt oxide nanoparticles (synthesized separately by microemulsion method) of appropriate amount 0, 1, 2, 5, 10 at% were added with the resultant yield. The mixer was ground well and annealed to 723 K for 3 hours in air. Finally, the synthesized powder was used for characterization.

3. Results and Discussion

3.1. X-Ray diffraction analysis

The crystal structure and phase purity of the samples were analyzed using PAN analtical X'pert PRO X-ray diffractometer. Fig. 1 shows the X-ray diffraction pattern of Co doped Mn_2O_3 nanosystem with different doping concentration (0, 1, 2, 5 and 10 at. %). The result reveals a cubic structure, as the diffraction peaks compared with the JCPDS file (JCPDS card No. 89-4836). From the XRD data, the lattice parameter is found to be a=9.408Å which is in good agreement with the JCPDS data and the results reported by S.Thota *et al*. (2010) [20]. The XRD pattern of 10 at. % Co doped Mn_2O_3, illustrates that the crystalline peaks corresponds to Mn_2O_3 in addition to that a secondary phase appears, which corresponds to (311) orientation of Co_3O_4, which might be due to the increase in concentration of Co ions above the solubility limit. The crystallite size (D) was estimated using Debye Scherrer's equation (Eqn. (1)).

$$D=\frac{K\lambda}{\beta\cos\theta}(m) \tag{1}$$

Where, β is the full width at half maximum (FWHM) of a diffraction peak, K is the shape factor ~ 0.9 and λ is the wavelength of the X-ray source(1.54 Å).

The calculated values of Co (0, 1, 2, 5, 10 at. %) doped α-Mn_2O_3 nanosystems were 27, 25, 20, 17 and 16 nm respectively. It was seen that the particle size reduces with increase of doping concentration, which may be due to quantum confinement in nanomaterials, the bulk system gets strained and this may be estimated for Co (0, 1, 5, 10 at. %) doped α-Mn_2O_3 nanosystems using Eqn. (2) as 0.011, 0.014, 0.022 and 0.029 respectively.

$$\eta=\left[\frac{\lambda}{t\cos\theta}-\beta\frac{\pi}{180}\right]\frac{1}{\tan\theta} \tag{2}$$

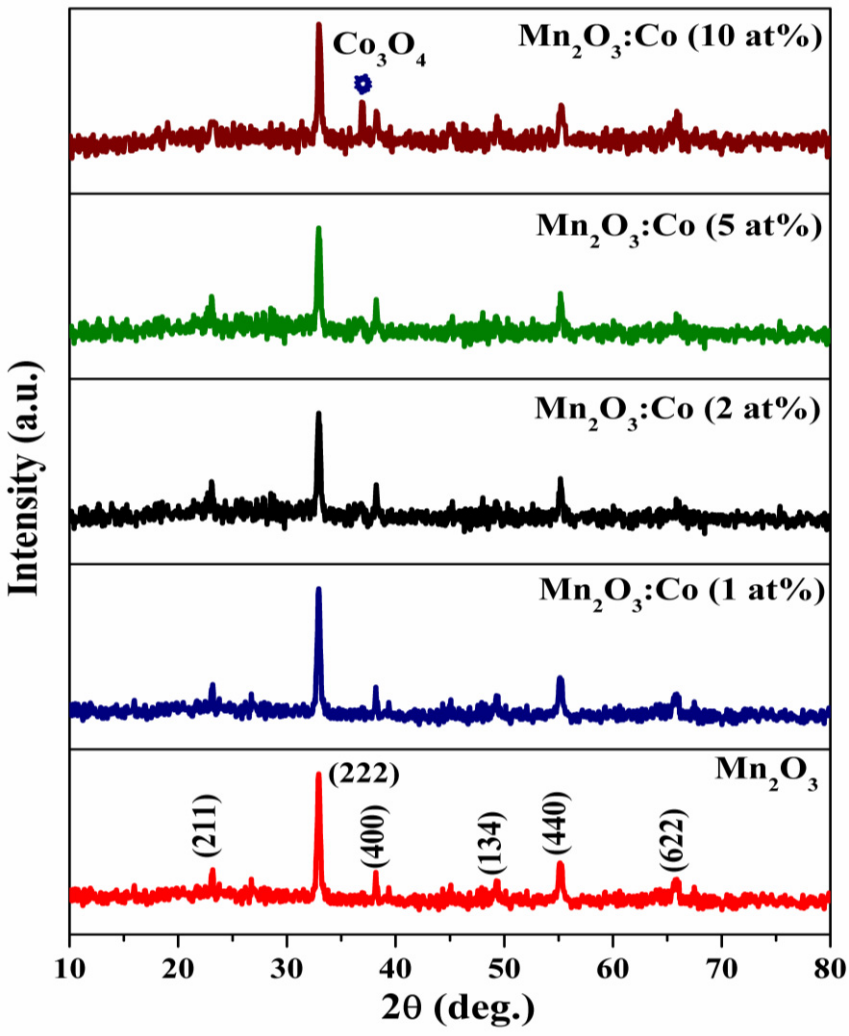

Fig.1 XRD pattern of α-Mn_2O_3: Co nanosystems

3.2. Scanning electron microscope and Energy dispersive X-ray analysis

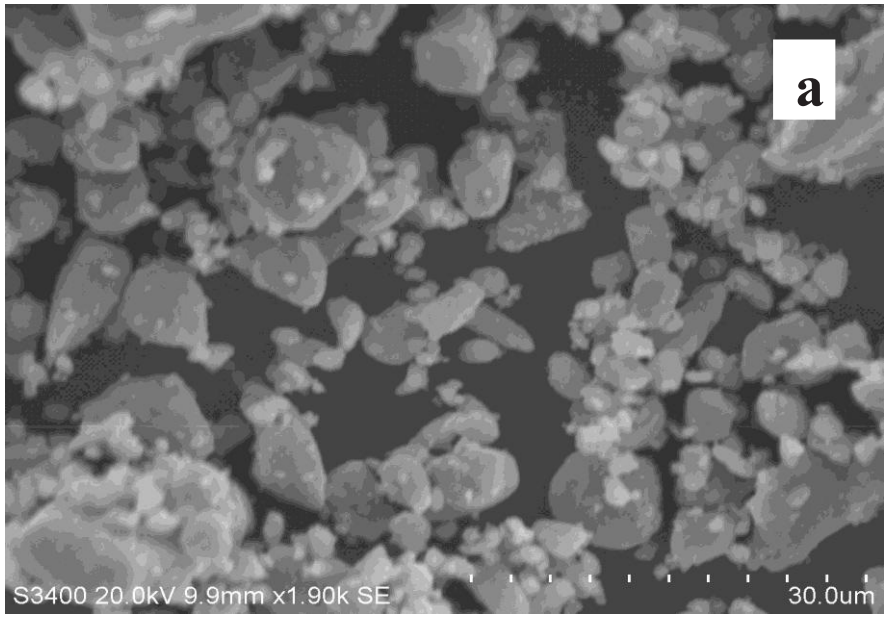

Fig. 2 (a) SEM image of Mn_2O_3 nanoparticles

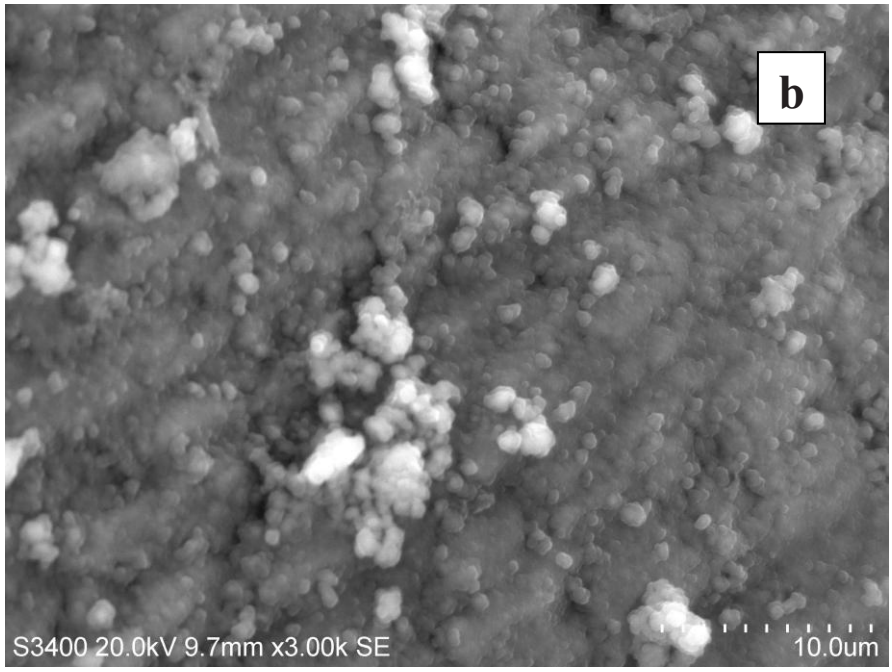

Fig. 2 (b) SEM image of cobalt (2 at. %) doped Mn_2O_3 nanoparticles

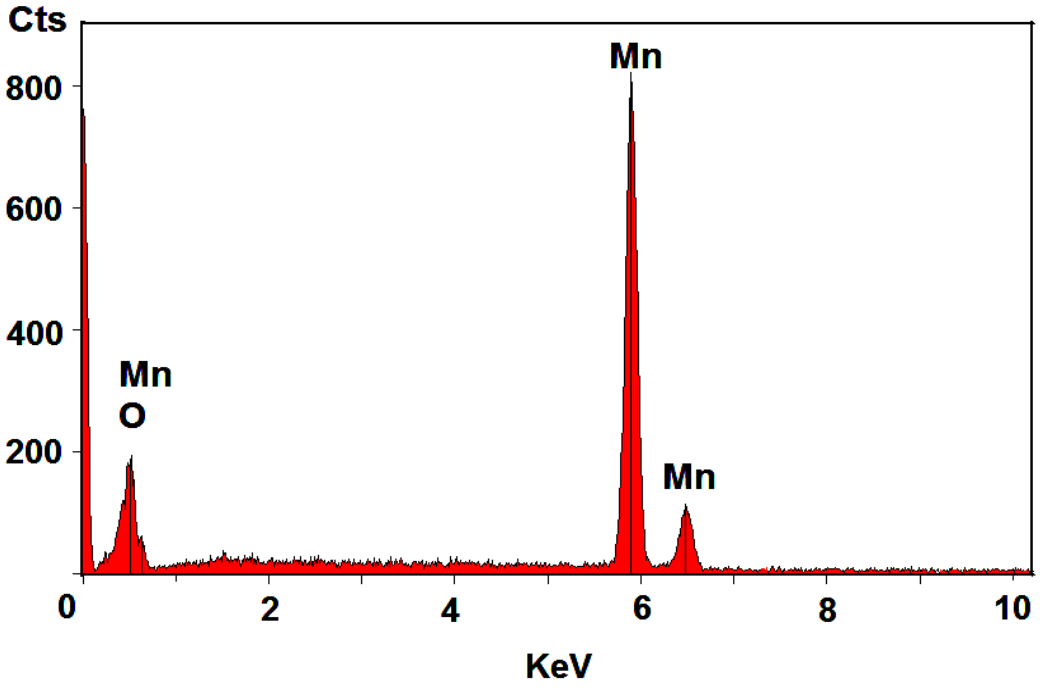

Fig. 3 (a) EDAX Spectrum of Mn_2O_3nanoparticles

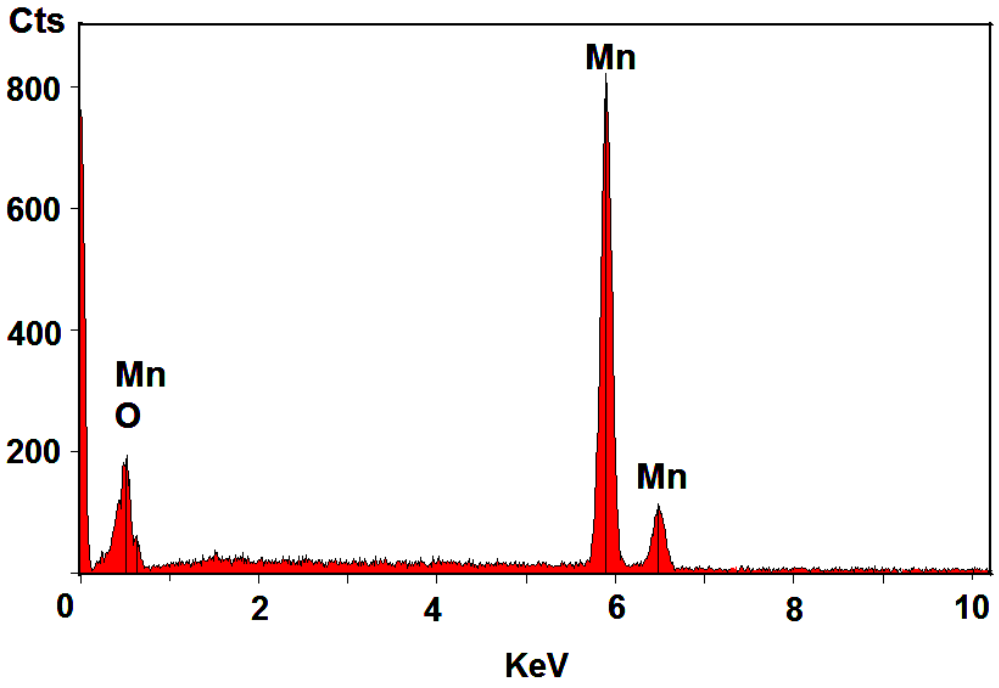

Fig. 3 (b) EDAX Spectrum of Co (2at. %) doped Mn_2O_3 nanoparticles

SEM with EDAX analysis examined the topographical and elemental composition of the synthesized nanosystem. SEM images of pure and Co (2 at. %) doped Mn_2O_3 nanoparticles are shown in Fig. 2(a) and (b).It is seen that, the Co doped Mn_2O_3 nanoclusters are not uniformly spread compared to undoped Mn_2O_3 nanoclusters. The Co doped Mn_2O_3 nanocluster appears like spherical shape and the diameter of nanoclusters ~ 2μm.

The spectrum of EDAX for pure Mn_2O_3 and Co (2 at. %) doped Mn_2O_3 are shown in Fig. 3(a) and (b). The spectrum shows the peaks corresponding to manganese, oxygen and manganese, cobalt, oxygen elements inferring that the prepared sample contains only Mn, O and Mn, Co, O elements respectively. The result confirms the purity of grown nanomaterial with no additive impurities.

3.3. UV-Vis analysis

The optical properties of prepared samples were studied by UV-Vis spectrometer. Fig. 4 show the absorbance spectra of Co doped Mn_2O_3 nanoparticles with different Co doping concentration. UV-Vis spectra were recorded in the transmission mode and it can be clearly seen that there is no visible absorption.

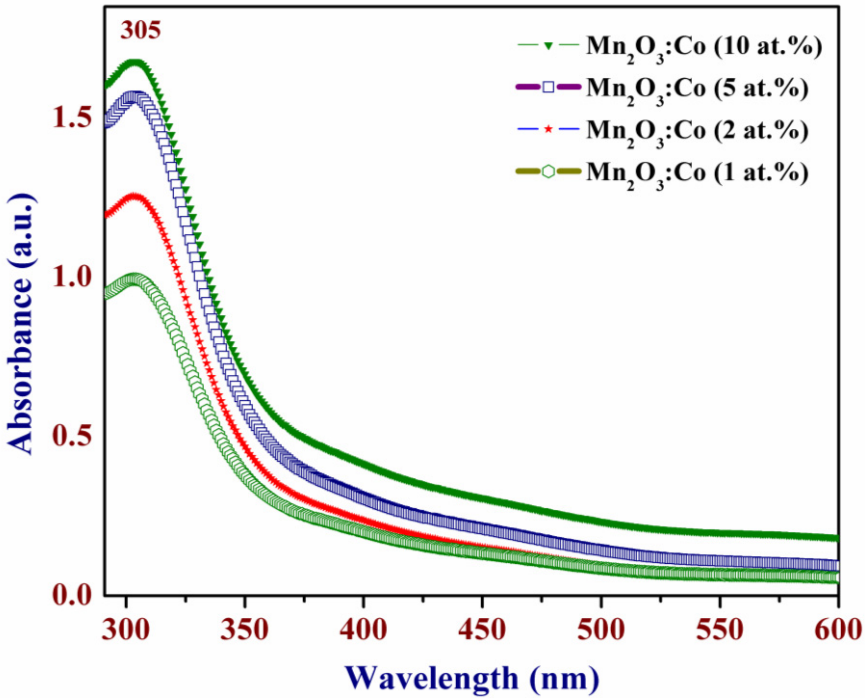

Fig .4 UV-Vis spectrum of cobalt doped Mn_2O_3 nanoparticles

The spectrum illustrates that a sharp peak occurs at ~ 305 nm, which is the effect of quantum confinement. By using this absorbance value in Planck's equation (Eqn. (3)), the bandgap energy was estimated as 4.06eV. The result shows that doping of cobalt in Mn_2O_3 increase the bandgap value that acquires the blue shift compared to bulk.

$$E = \frac{hc}{\lambda} \text{ (eV)} \tag{3}$$

Where, h is Planck's constant (6.626×10^{-34} Js). c is velocity of light (3×10^{8} m s^{-1}). λ is the wavelength corresponding to the sharp absorbance.

3.4 Fourier transforms infrared spectroscopy analysis

In molecules and crystals, the atoms or ions are connected by chemical bonds. These systems can be set into vibration depending on the elements and type of bond present. This vibrational frequencies determined by the mass of atoms (atomic weight) and bond strengths. The mechanical molecular and crystal vibration are at very high frequencies ranging from 10^{12} to 10^{14} Hz, which is in the Infrared (IR) regions of the electromagnetic spectrum. When vibrational frequencies are in resonance, impinging beam of infrared electromagnetic radiation is coupled. These absorption frequencies represent vibrations of the chemical bond, specific type of bond and the group of atoms involved in the vibration.

In the infrared experiment, the intensity of a beam of infrared radiation is measured before and after interacts with the sample as a function of light frequency. A plot of relative intensity verses frequency is the 'infrared spectrum'. When the intensity-time output of the interferometer is subjected to a Fourier transform to convert it into the infrared spectrum (intensity-frequency). FTIR spectrum of cobalt doped Mn_2O_3 nanosystem is given in Fig. 5.

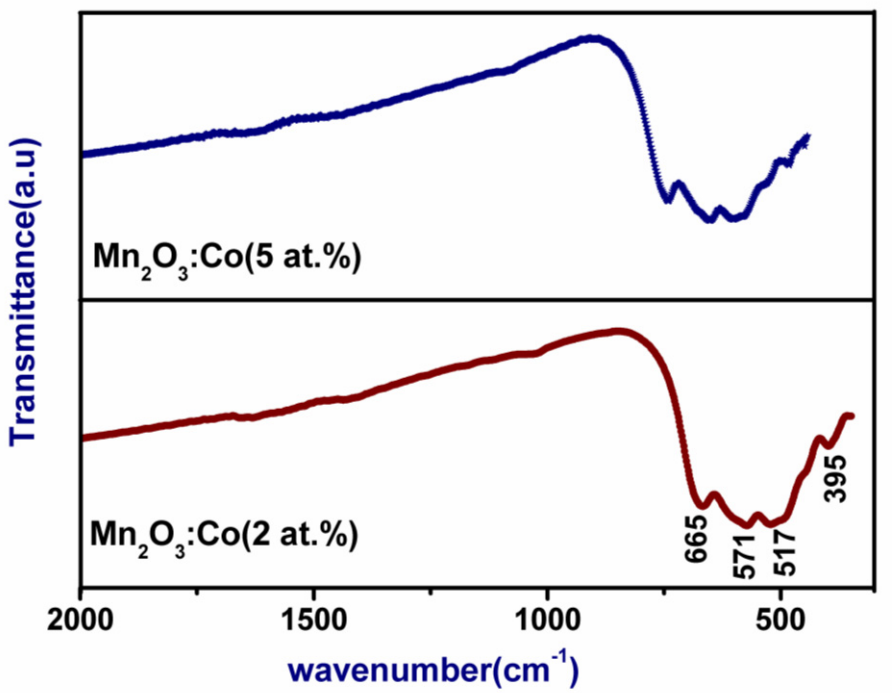

Fig. 5 FTIR spectrum of cobalt doped Mn_2O_3 nanoparticles

The functional groups of cobalt doped Mn_2O_3 nanoparticles are given in Table 1. The results are in good agreement with literature [21]. The peaks around 500 and 600 cm^{-1} denote the Mn-O stretching mode.

Table 1. FTIR data for cobalt doped Mn_2O_3 nanoparticles

Functional groups	Transmittance (cm^{-1})
C-CN bond	395
ν(Mn-O) mode of stretching	517, 571
C-OH stretching	665

3.5 Electron Paramagnetic Resonance

In Electron Paramagnetic Resonance (EPR) spectra of Co doped Mn_2O_3 nanoparticles, the broad line has a derivative line with a width in the range ~300-380 mT at room temperature. The crystal structure of the Mn_2O_3 crystal revealed that Mn^{3+} ions ($3d^4$, s = 2) are under tetragonaly distorted octahedral environments of O^{2-} ions [19]. A doubly degenerate ground state under an octahedral field because of tetragonal distortion splits into two singlets.

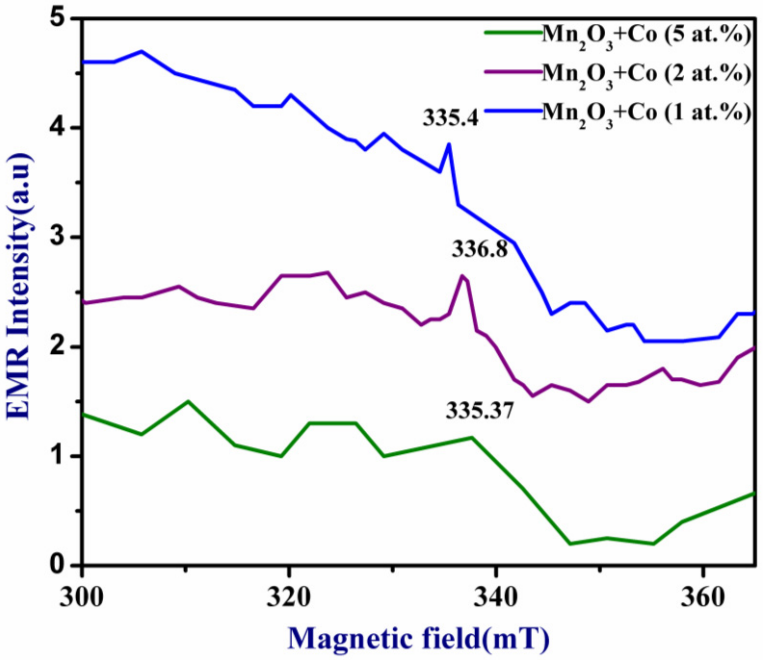

Fig.6. EPR spectrum of Mn_2O_3: Co nanosystem

In the EPR spectrum, there is splitting of lines corresponding to Mn_2O_3 nanoparticles. This may be due to the addition of cobalt ions. EPR spectrometer was operated at constant frequency (ν = 9.3 GH_Z), while magnetic field is swept. Fig.6 illustrates that with increase in Co concentration the peak shift towards

higher magnetic field due to exchange narrowing of the signal. The Lande-g factor was calculated (Table 2) corresponding to magnetic field shift using the Eqn (4).

$$g = \frac{h\nu}{\mu_B B_0} \tag{4}$$

Where, h is Planck's constant. ν is operating frequency of EPR spectrometer. μ_B is Bohr magneton and B_0 represent the magnetic field shift.

Table 2 Lande-g factor for Co doped Mn_2O_3 nanoparticles by EPR measurements

Atomic percentage of Co doping with Mn_2O_3 nanoparticles	Magnetic field (mT)	Lande-g factor
1	337.5	1.97
2	336.8	1.98
5	335.3	1.99

These results show that the material is most probably having paramagnetic or ferromagnetic behaviour. However, EPR study does not confirms the exact magnetic behaviour of a nanosystem.

3.5 Guoy's method

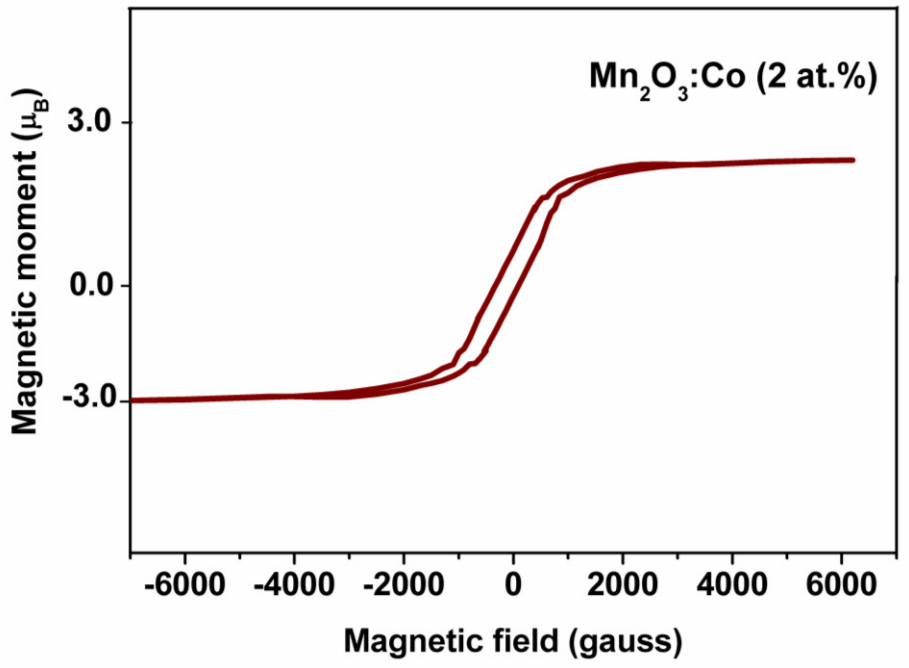

Fig.7 (a) Hysteresis loop of Co (2 at.%) doped Mn_2O_3 nanoparticles

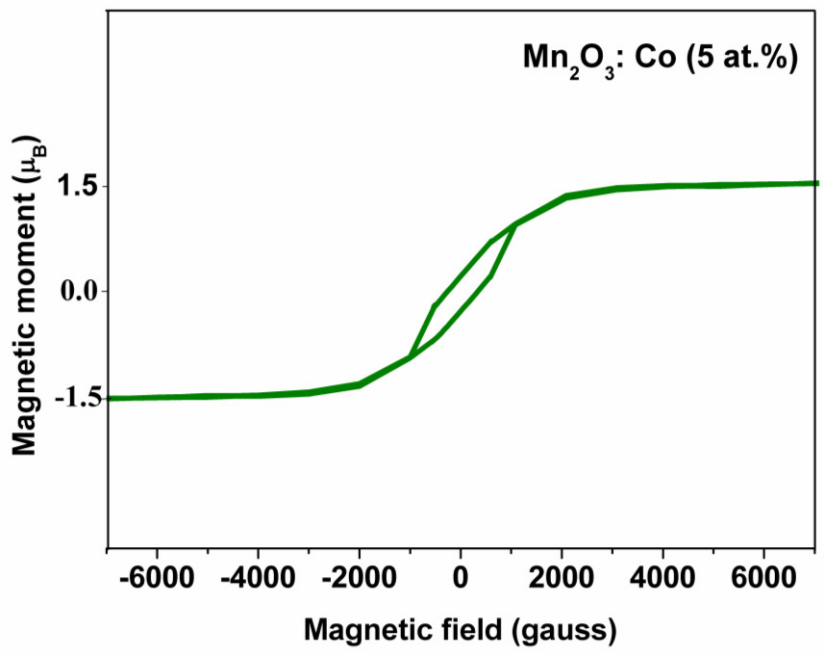

Fig.7 (b) Hysteresis loop of Co (5 at.%) doped Mn_2O_3 nanoparticles

Hysteresis loops (Fig.7 (a) and (b)) were drawn to study the magnetic properties of prepared samples by Guoy's method. The result shows, Co (1 at. %) doped Mn_2O_3 nanoparticles has the high value magnetic moment ($3.5\mu_B$) which is close to magnetic moment of manganese ($\sim 5\mu_B$). This indicates that there is a raise in transition temperature of Mn_2O_3. However, the value of magnetic moment for higher atomic percentage of Co doping with Mn_2O_3, reduces gradually and reaches zero with increase in percentage of doping. Though, addition of ferromagnetic ions (cobalt) with antiferromagnetic material (Mn_2O_3), results antiferromagnetic nature due to the orientation of spin. (i.e.) antiferromagnetism at room temperature.

It is observed that the ferromagnetic T_C might have been increased from 90K to some higher value, due to the large value of magnetic moment. From the hysteresis loop coercivity, retentivity and magnetic moment were calculated and depicted in Table 3.

Table 3. Magnetic parameters from hysteresis loop

Nanomaterial	Coercivity (G)	Retentivity (emu/gm)	Magnetic moment (μ_B)
Mn_2O_3:Co (1at. %)	221	0.33	3.50
Mn_2O_3:Co (2at. %)	251	0.22	2.62
Mn_2O_3:Co (5at. %)	316	1.42	1.49

4. Conclusion

Co doped Mn_2O_3 nanoparticles were synthesized by chemical route. The structure of the nanoparticles, cell parameters and strain were calculated from the XRD results. Morphology of the nanosystem have been studied using SEM and EDAX, confirms the presence of chemical elements in the nanosystem. The optical properties were studied using UV-Vis and FTIR spectrometers. From the UV-Vis absorbance, band gap values were calculated and FTIR confirms the presence of Mn-O bonding. Magnetic studies were studied by using EPR and Guoy's method. The EPR measurement for Co doped Mn_2O_3 nanosystem shows the possibility of paramagnetism / Ferromagnerism. But, Guoy's method clearly confirms the presence of ferromagnetism in lower atomic percentage of Co doped Mn_2O_3 nanoparticles at room temperature. The obtained values of magnetic moment are compared with bulk and theoretical values. So, it has been concluded that addition of Co in Mn_2O_3 will not enhance it's intrinsic magnetic properties. As Co is a magnetic impurity, there was a raise in ferromagnetic T_c of Co doped Mn_2O_3 nanosystem.

References

[1] Si, PZ., Li, D., Choi, CJ., Li, YB., Geng, DY., Zhang, ZD., 2007. Large coercivity and small exchange bias in Mn_3O_4 /MnO nanoparticles. Solid State Communications 142, 723-6.

[2] Park, J., Kang, E., Bae, CJ., Park, JG., Noh, HJ., Kim, JY., et al., 2004. Synthesis, characterization, and magnetic properties of uniform –sized MnO nanospheres and nanorods. Journal of Physical Chemistry B 108 , 13594-8.

[3] Ahmad, T., Ramanujachary, KV., Samuel, E., Ganguli, AK., 2004. Nanorods of manganese oxalate: a single source precursor to different manganese oxide nanoparticles (MnO, Mn_2O_3, Mn_3O_4). Journal of Materials Chemistry 14, 3406-10.

[4] Olmos, AV., Redon, R., Osorio, ALF., Saniger, JM., 2005. Room-temperature synthesis of Mn_3O_4 nanorods. Applied Physics A 81, 1131-4.

[5] Folch, B., Larionova, J., Guari, Y., Guerin, C., Mehdi, A., Reye, C., 2004. Formation of Mn_3O_4 nanoparticles from the cluster $[Mn_{12}O_{12}(C_2H_5COO)_{16}(H_2O)_3]$ anchored to hybrid mesoporous silica. Journal of Materials Chemistry 14, 2703-11.

[6] Yang, LX., Zhu, YJ., Tong, H., Wang, WW., Cheng, GF., 2006. Low temperature synthesis of Mn_3O_4 polyhedral nanocrystals and magnetic study. Journal of Solid State Chemistry 179, 1225-9.

[7] Zhang, YC., Qiao, T., Hu, XY., 2004. Preparation of Mn_3O_4 nanocrystallites by low-temperature solvothermal treatment of γ-MnOOH nanowires. Journal of Solid State Chemistry 177, 4093- 7.

[8] Lei, S., Tang, K., Fang, Z., Sheng, J., 2007. One-step synthesis of colloidal Mn_3O_4 and γ-Fe_2O_3 nanoparticles at room temperature. Journal of Nanoparticle Research 9, 833-40.

[9] Zunger, A., Wanger, S., 1993. Special issue on research opportunities in photovoltaic semiconductors-foreword. Journal of Electronic Materials 22, 1-1.

[10] Makovec, D., Drofenik, M., Znidarsic, A., 2001. Sintering of MnZn-ferrite powders prepared by hydrothermal reactions between oxides. Journal of the European Ceramic Society 21, 1945-9.

[11] Ramachandran, R., Rashmi., 2002. Preparion and characterization of manganous manganic oxide (Mn_3O_4). Journal of Materials Science - Materials in Electronics 13, 257-62.

[12] Drofenik, M., Znidarsic, A., Kristl, M., Kosak, A., Makovec, D., 2003. Dispersant-assisted hydrothermal synthesis of MnZn ferrites from raw oxides. Journal of Materials Science 38, 3063-7.

[13] Zhang, X., Yue, L., Wan, M., Zheng, Y., 2010. Synthesis of porous manganese oxides bars via a hydrothermal-decomposition method. Materials Chemistry and Physics 124, 831–4.

[14] Hassan, MS., Amna, T., Pandeya, DR., Hamza, AM., Bing, YY., Kim., HC., et al., 2012. Controlled synthesis of Mn_2O_3 nanowires by hydrothermal method and their bactericidal and cytotoxic impact:a promising future material. Applied Microbiology and Biotechnology 95, 213–22.

[15] Francis, TM., Lichty, PR., Weimer, AW., 2010. Manganese oxide dissociation kinetics for the Mn_2O_3 thermochemical water-splitting cycle. Part1:Experimental. Chemical Engineering Science 65, 3709-17.

[16] Ju, SH., Kim, DY., Koo, HY., Hong, SK., Jo, EB., Kang, YC., 2006. The characteristics of nano-sized manganese oxide particles prepared by spray pyrolysis. Journal of Alloys and Compounds 425, 411-5.

[17] Zhiwen, C., Shuyuan, Z., Shun, T., Fanqing, L., Jian, W., Sizhao J., et al., 1997. Preparation and electron spin resonance effect of nanometer -sized Mn_2O_3. Journal of Crystal Growth 180, 280-3.

[18] Si, PZ., Zhang, ZD., 2009. Large coercivity in antiferromagnetic Mn_2O_3/ Mn_5O_8 and MnO/Mn nanoparticles. International Journal of Modern Physics B 23, 3895-901.

[19] Mukherjee, S., Pal, AK., Bhattacharya, S., Raittila, J., 2006. Magnetism of Mn_2O_3 nanocrystals dispersed in a silica matrix: Size effects and phase transformations. Physical Review B 74, 104413-1-104413-10.
[20]Thota, S., Prasad, B., Kumar, J., 2010. Formation and magnetic behaviour of manganese oxide nanoparticles. Journal of Materials Science and Engineering B 167, 153- 60.
[21] Askarinejad, A., Morsali, A., 2009. Direct ultrasonic-assisted synthesis of sphere-like nanocrystals of spinel Co_3O_4 and Mn_3O_4. Ultrasonics Sonochemistry 16, 124-31.